Statistical Analysis of Variation in Laboratory Growth of Carbon Nanotube Forests and Recommendations for Improved Consistency

C. Ryan Oliver,[†,§] Erik S. Polsen,[†,§] Eric R. Meshot,[†,∥] Sameh Tawfick,[†,‡] Sei Jin Park,[†] Mostafa Bedewy,[†] and A. John Hart[†,‡,*]

[†]Mechanosynthesis Group, Department of Mechanical Engineering, University of Michigan, 2350 Hayward Street, Ann Arbor, Michigan 48109, United States and [‡]Department of Mechanical Engineering, Massachusetts Institute of Technology, Cambridge, Massachusetts 02139, United States. [§]C.R.O. and E.S.P. contributed equally. [∥]Current address: Lawrence Livermore National Laboratory, 7000 East Avenue, Livermore, California 94550, United States.

ABSTRACT While many promising applications have been demonstrated for vertically aligned carbon nanotube (CNT) forests, lack of consistency in results (*e.g.*, CNT quality, height, and density) continues to hinder knowledge transfer and commercialization. For example, it is well known that CNT growth can be influenced by small concentrations of water vapor, carbon deposits on the reactor wall, and experiment-to-experiment variations in pressure within the reaction chamber. However, even when these parameters are controlled during synthesis, we found that variations in ambient lab conditions can overwhelm attempts to perform parametric optimization studies. We established a standard growth procedure, including the chemical vapor deposition (CVD) recipe, while we varied other variables related to the furnace configuration and experimental procedure. Statistical analysis of 280 samples showed that ambient humidity, barometric pressure, and sample position in the CVD furnace contribute significantly to experiment-to-experiment variation. We investigated how these factors lead to CNT growth variation and recommend practices to improve process repeatability. Initial results using this approach reduced run-to-run variation in CNT forest height and density by more than 50%.

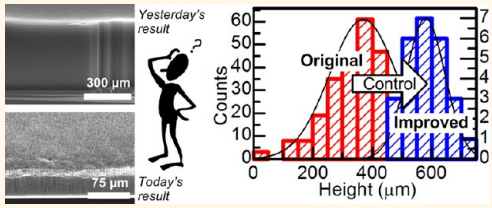

KEYWORDS: carbon nanotubes · chemical vapor deposition · nanomaterials · variation · error · process control

Attaining consistent results is essential to the transfer of new materials processing methods from lab to lab and from lab to industry. While lab-scale research efforts often focus on concept demonstration rather than quality control, a lack of process consistency can hinder knowledge transfer and lead to inefficient use of resources in attempting to replicate published data. In the authors' opinion, this issue is particularly relevant to nanomaterials research, as many exciting lab-scale demonstrations now demand focus on detailed engineering and manufacturing research to create commercial value.[1] Moreover, the parameter space for nanomaterials synthesis process conditions is large and often incompletely known, which limits rigorous understanding and the ability to extrapolate research findings to new processes and applications.

For example, commercialization of new materials and devices incorporating vertically aligned carbon nanotubes (CNTs), or CNT "forests", requires precise control of structural attributes (*e.g.*, CNT diameter, quality, density, and alignment) as well as process performance (*e.g.*, growth rate, reaction efficiency). This control is essential to implementing principles of scale-up, and it is relevant for designing CNT forests to achieve target performance for applications such as thermal interfaces[2−4] and electrical interconnects.[5−7] There is a wealth of knowledge regarding the influence of several factors governing CNT growth by chemical vapor deposition (CVD), including hydrocarbon gas chemistry,[8] process conditions (*e.g.*, pressure, temperature),[9] moisture content,[10] reactor wall conditions,[11] and other factors.[12,13] Regardless, experts still accept that CNT forest growth is highly nonrepeatable under typical laboratory conditions.

This nonrepeatability suggests that there are "hidden" factors that influence CNT

* Address correspondence to ajohnh@umich.edu.

Received for review January 30, 2013 and accepted March 6, 2013.

Published online March 06, 2013
10.1021/nn400507y

growth, such as ambient conditions and differences in standard procedures, the details of which are sometimes difficult to learn from the literature. Moreover, limitations in consistency of CNT growth have, in the authors' opinion, led to excessive trial-and-error process tuning rather than systematic approaches guided by fundamental understanding. Researchers frequently endeavor to use low-cost atmospheric pressure CVD systems such as tube furnaces because they are easy to set up and operate, and sometimes perform research outside of a clean room environment in order to reduce facility cost and maintenance constraints. At the same time, this practice increases the risk of process variation, unless sources of variation are understood and appropriate controls are implemented.

For instance, it is well known that CNT growth can be influenced by ppm-level changes in the concentration of H_2O vapor (moisture) within the CVD reaction chamber.[14−16] However, it is not widely known how ambient humidity levels affect the CNT synthesis conditions. One example is the intrusion of air into an open CVD chamber during sample exchange or the retention or permeation of moisture in porous system components. Due to rapid or seasonal weather changes, ambient humidity can fluctuate by 1−10 000 ppm, compared to the 100 ppm moisture level first shown to influence CNT forest growth.[10,14] Moreover, how moisture and other trace impurities/additives, such as oxygen[17] and alcohols,[18] affect CNT growth is partially determined by the hydrocarbon and hydrogen mixture in the reactor, which is also known to evolve along the length of the tube due to thermally activated reactions.[19,20] Therefore, without rigorous methods to identify and eliminate sources of moisture and other potential sources of process variation, "hidden" conditions may influence CNT synthesis in an unknown way.

We present a comprehensive statistical analysis of the sources of variation in the growth of CNT forests, using a conventional tube furnace operated under atmospheric pressure. For this study, we defined a standard CNT growth recipe, introduced controlled perturbations of several operational variables, and monitored uncontrolled factors such as ambient conditions. We found that ambient conditions (humidity and barometric pressure) contribute significantly to variations in CNT forest height and density and communicate to the process *via* choice of reactor materials and load procedures. In addition, substrate samples placed at the first (upstream) position in the furnace consistently resulted in taller and denser CNT forests than those downstream. A separate series of experiments identified that the moisture level in the reactor influences dewetting of the thin-film catalyst, which in turn influences the CNT density, and that polytetrafluoroethylene (PTFE) gas supply lines can absorb significant amounts of moisture and, therefore, contaminate the high-purity source gases. Last, we demonstrate a 50% reduced coefficient of variation by modifying the CVD system to isolate it from ambient conditions and establish consistent automated sample placement, while remaining in an uncontrolled lab environment.

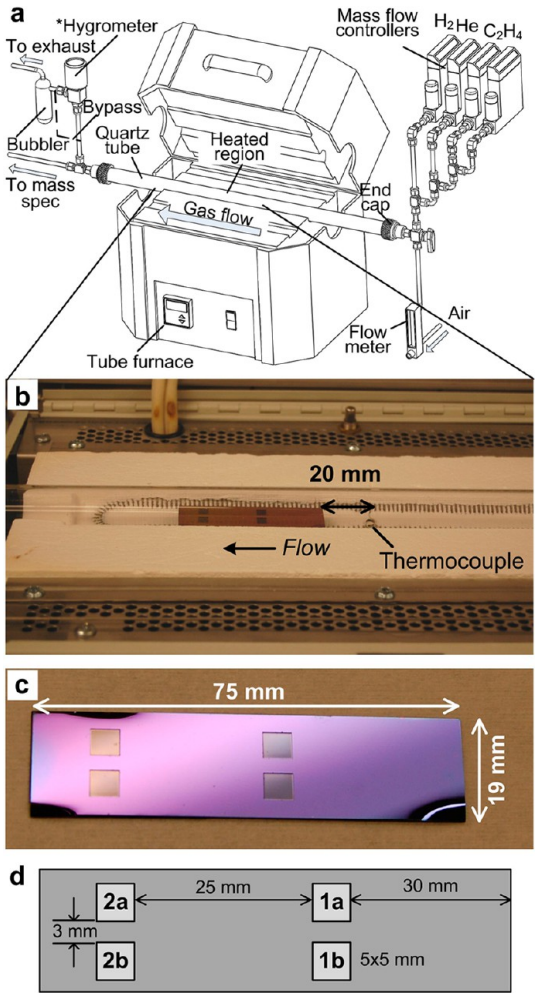

Figure 1. CVD system and sample configuration for reference growth study. (a) Schematic of CVD tube furnace system with hygrometer at output. (b) Image of silicon wafer "boat" inserted into the quartz tube and positioned in the furnace for a growth experiment. (c) Image of the boat with the cavities for sample placement. (d) Schematic of boat indicating dimensions and encoding of sample positions with respect to position along the tube (1, 2) and side (a, b). Position 1 is upstream relative to position 2.

STANDARDIZED CNT GROWTH PROCEDURE

In order to study the sources of variation in CNT (all references to CNT growth in this paper are referring to multiwalled nanotubes per our typical conditions[21]) forest synthesis, we used an atmospheric CVD system (Figure 1a) and defined a "reference" procedure, consisting of a list of operational variables (Table 1) and growth (Table 2) and baking (Table 3) recipes. The list of operational variables was constructed from known possible factors suspected to influence the outcome

TABLE 1. Operational Parameters of Reference CNT Growth Procedure

process variable	set value	control method
substrate dimensions	5 × 5 × 0.5 mm	wafer etched
samples per run	4	counted
boat dimensions	75 × 19 × 0.5 mm	etched by DRIE
boat location	60 mm from tube end	alignment ring on insertion rod
experiments/week	2	Monday, Friday
tube placement	center of furnace	alignment mark
sample placement	refer to Figure 1	etched into Si boat
line pressure	20 psi	gauge reading
recipe	refer to Table2	computer (LabView)
alumina thickness	14—15 nm	AFM
Fe thickness	2.9—3.1 nm	AFM
bubbler liquid level	10 mm	visually verified

TABLE 2. CNT Growth Recipe

process time	step duration (min)	He	H_2	C_2H_4 (sccm)	set temperature (°C)
5	5	400	100	100	25
10	5	1000	0	0	25
15	5	400	100	0	25
25	10	400	100	0	775
35	10	400	100	0	775
45	10	400	100	100	775
50	5	1000	0	0	25

TABLE 3. Reactor Baking Recipe

time (min)	air (sccm)	set temperature (°C)
5	1000	25
10	1000	875
20	1000	875
5	1000	25

of a CNT growth experiment, in addition to the standard parameters of the growth recipe. For example, we had previously hypothesized that the original location on the source wafer from which the catalyst growth substrate was sampled could influence the CNT growth outcome. Also, we had observed that CNT growth results (*e.g.*, height, density) were different between the first experiment and subsequent experiments performed using the same CVD system on the same day. The growth recipe was based on our experience[22,23] and is consistent with processes used by several other groups.[14,24,25]

The procedure began with sample preparation. Two clean silicon (100) wafers, having 300 nm of thermally grown SiO_2, were coated with 10 nm of Al_2O_3, followed by 1 nm of Fe (measured to be 3 nm by AFM after exposure to air), using e-beam evaporation. The wafers were loaded simultaneously into the chamber and coated in the same deposition run. Then each wafer was diced into 5 × 5 mm samples, which were numbered and cataloged based on their original location on the wafer, in order to later identify CNT growth variation that arose from nonuniformity in catalyst thickness across the wafer. Half of the samples from each wafer were randomly selected and put into separate polystyrene Petri dishes, yielding four dishes. Two of the dishes, corresponding to half of each wafer, were placed inside a desiccator, while the other two dishes were stored outside of the desiccator, in the lab ambient. This separation of samples was done to investigate the effects of variations in the laboratory environment on the catalyst and the effects of variations in user practices for storing and handling samples. Specifically, we wanted to investigate if absorption/adsorption of water to the samples was a significant source of moisture in the reaction chamber during the CVD process. Thus, the desiccator was utilized to provide a dry environment for half of the samples.

We then determined a plan for experiments that would evaluate the influence of the operational variables on the height and density of the resultant CNT forests. Using standard *a priori* statistical power analysis (Optimal Design software[26]), we estimated that 70 experiments would be needed to achieve statistically significant results (power = 0.85). We wanted to be able to detect a 40 μm shift in height caused by any variable being investigated, which we call the effect size. We calculated the number of experiments necessary to capture the effect size with 4 samples per experiment, which equaled 70 experiments.

Prior to beginning the series of "reference growth" experiments, each system component that was used for process control and/or measurement was calibrated, and nominal values (baseline measurements) expected to remain unchanged for all experiments were collected. We collected baseline measurements from each of our sensors (*i.e.*, mass flow controllers, furnace thermocouple, exhaust bubbler, mass spectrometer, mass balance, laser displacement sensor for CNT height measurement, e-beam deposition crystal monitor, desiccator humidity gauge, ambient data logger, and Raman spectrometer) to ensure that each was within the calibration specification. We purged our gas supply lines (connecting the tanks to the CVD system) by evacuating each line (<10 Torr) while flowing 500 sccm He, 500 sccm H_2, and 200 sccm C_2H_4 for 30 min. Each gas line was approximately 8 m long, with a 10 mm inner diameter, thus constituting an internal volume of approximately 630 cm^3. The tube furnace temperature profile (Figure S1) was measured by inserting a thermocouple through an Ultratorr (Swagelok) fitting attached to the furnace tube end-cap (see Methods). To ensure consistent operation over the entire study, the baseline measurements and calibrations were performed again and compared to the initial baseline ($N = 0$), at experiment numbers $N = 35$ and $N = 70$. No corrections were needed throughout the study.

Each experiment began by randomly selecting one sample (*i.e.*, a 5 × 5 mm substrate) from each of the four

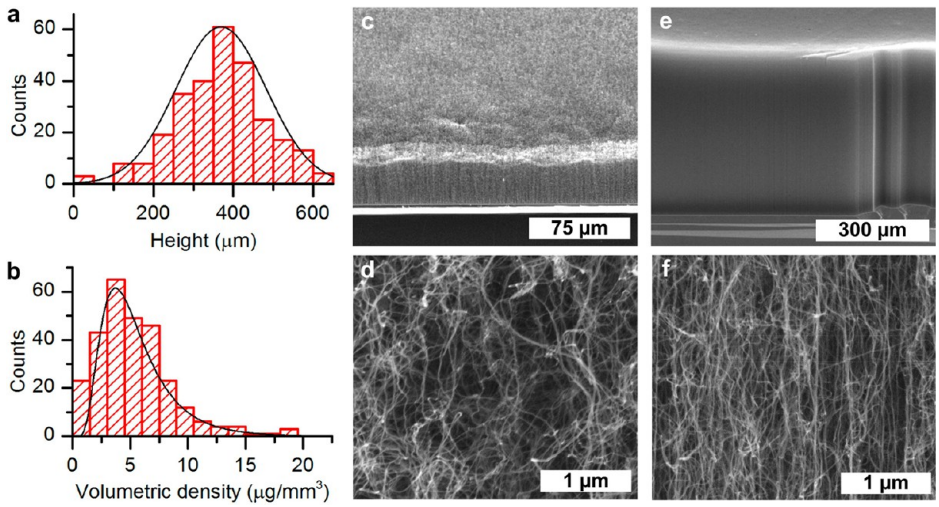

Figure 2. Variation in CNT height and density during the reference growth study. (a) Histogram of height measurements taken from 280 samples for the complete study. (b) Histogram of volumetric density measurements taken from 280 samples for the complete study. (c) SEM image of the sidewall of a short CNT forest. (d) SEM image of the sidewall of a tall CNT forest. (e, f) Corresponding close-up images of the forests, showing clear differences in CNT alignment and density.

Petri dishes, weighing the samples using the microbalance (taking the average value of 4 measurements for each sample), measuring the sample dimensions using a set of digital calipers, and placing the samples in cavities on the etched silicon carrier substrate ("boat") shown in Figure 1c. Samples taken from the desiccator were placed in positions 1a and 2b on the boat, and samples stored in ambient were placed in positions 1b and 2a. On alternate experiment days, the relative positions were switched. Then, the boat was loaded into the tube such that the leading edges of samples 1a and 1b were 50 mm downstream of the center of the furnace (the location of the control thermocouple). On the basis of our previous work, this was the general "sweet spot" for this recipe.

The furnace temperature, gas flows, and process sequence were controlled and recorded using a custom LabView program. During each experiment the gases at the output of the furnace tube were sampled using an inline quadrupole mass spectrometer (Pfeiffer OmniStar GSD 301) (Figure S2). At the conclusion of the growth sequence, the boat was removed from the tube, each sample was weighed, and the mass of each CNT film was calculated by subtracting the mass of the corresponding catalyst substrate before CNT growth. Height measurements were averaged across five points around the chip using a laser displacement sensor, and the volumetric and areal density of each sample was calculated using the measured dimensions, height and mass. Further details of characterization are given in the Methods section.

After each experiment, the empty boat was placed in the tube, and the system was heated to 875 °C under a flow of dry air and held for 30 min. The purpose of this step was to oxidize carbon that was deposited on the quartz tube interior and boat during the CNT growth experiment and, thus, to keep the quartz tube in a consistent condition over the course of the study. The air bake ("bake-out") after the first daily experiment was done directly before the second daily experiment, whereas the bake-out after the second daily experiment occurred directly after the second daily experiment. As a result, the tube and boat were exposed to the lab atmosphere prior to the first daily experiment, which allowed us to study how storing the reactor tube in ambient conditions affects CNT growth.

RESULTS AND DISCUSSION

Using the reference growth procedure, we performed 70 CNT growth experiments, each with four substrate samples, therefore totaling 280 CNT forest samples. For the first 32 experiments, two experiments were performed each day, two days a week. For the remainder of the study, we performed two experiments per day, one day a week. This resulted in a total study time of approximately 6 months.

Histograms of height and density for the full population of samples are shown in Figure 2. The coefficient of variation for height and density are 31% and 63%, respectively. Frankly, we had tolerated these variations throughout our previous research and had noticed that, under the same recipe, CNT forests grew taller in the winter months than the summer months, presumably due to significant changes in ambient humidity/temperature at our location (Michigan, USA). However, this was the first time we quantified the variation, and to our knowledge it is the first time this has been quantified and explained in the literature.

Ambient conditions (temperature, humidity, barometric pressure) fluctuated over a wide range during the course of the study (Figure 3), as measured using

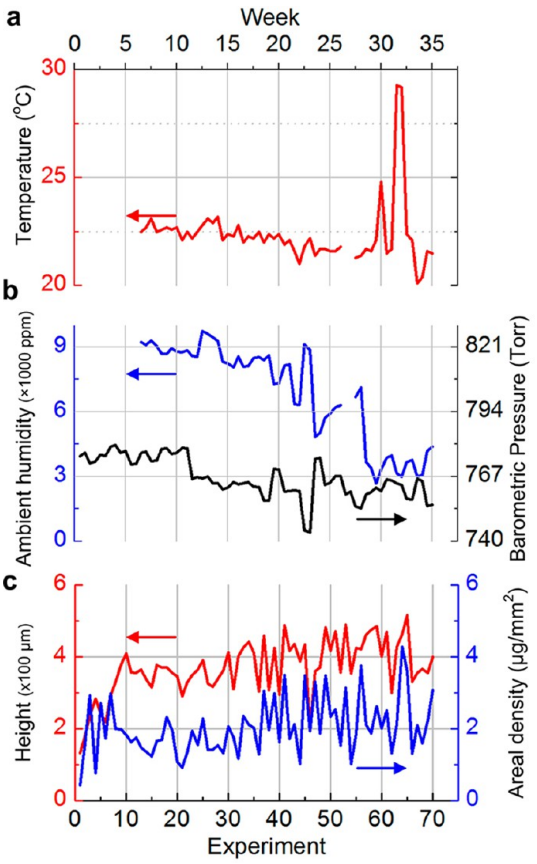

Figure 3. Ambient laboratory conditions. Plots of (a) temperature and (b) humidity and barometric pressure for each experiment. Data points represent the value in the lab at the beginning of the experiment with a start date of 7/23/2010. Temperature and humidity data were not collected for weeks 0−6. Data were lost for week 27 due to a sensor malfunction. (c) Plot of CNT forest height and areal density for each experiment.

an electronic data logger placed next to the reactor in the lab. Comparing the trends of height and density to ambient conditions appeared to validate our hypothesis that ambient factors contributed to growth variation. Sharp changes in humidity appear to cause changes in CNT height and density, for example, between weeks 20 and 25.

Further trends are revealed by separating the full data set according to the order of experiments on each day of the study, as well as the position of the sample along the reactor tube, as shown in Figure 4. Significant variation is present in both subsets of first and second daily experiments (Figure 4a,b), yet the sample position and experiment order present well-defined differences in mean CNT height and areal mass density (Figure 4c,d). Moreover, *via* scatter plots of height and density *versus* ambient humidity (for the same respective experiment of the day and sample position), we noted an apparently parabolic relationship with ambient humidity.

We compared the quality of fitness values for linear and parabolic relationships between humidity and the measured CNT forest height, and the parabolic relationship showed an adjusted R^2 value twice that for a linear relationship. However, we acknowledge that the multivariate nature of the experiments results in a weak relationship with the data, as pointed out by a low Pearson's correlation coefficient for these fits. We also note chemical reaction rates typically exhibit a parabolic relationship with control variables, and so it should be expected that both too little and too much water would not be best for the chemical reactions that produce CNTs. The parabolic relationship is consistent with previous studies of CNT growth where much smaller amounts of moisture were added directly to the CVD furnace.[10] Therefore, although there is significant scatter in this data, it suggested there may be optimal humidity level(s) that maximizes CNT height and/or density for a particular growth recipe.

In order to more rigorously identify the causes of CNT growth variation, we performed a multivariate linear regression among height, density, and eight of the operational and process variables (Table 1). The correlation coefficients between CNT growth results and five selected operational variables are shown in Table 4. Statistical significance was determined using the *p*-value criterion, which determines if observed variation is due to chance or due to a known factor that may or may not be controlled. We used a widely accepted threshold of $p = 0.05$. A *p*-value greater than 0.05 cannot conclude that the factor did not influence the measured outcome, and a *p*-value less than 0.05 indicates that the factor influenced the measured results. We also computed the *r*-value, called Pearson's correlation coefficient, to provide the degree of correlation. An *r*-value of 1 indicates perfect correlation, while an *r*-value of 0 indicates no correlation; the sign of the *r*-value indicates the direction of relationship (inverse or direct). Using the *p*-values, we found statistically significant correlations: height was correlated to ambient humidity ($p = 0.00$, $r = -0.22$) and sample location in the furnace ($p = 0.01$, $r = 0.16$), and areal density was correlated to ambient humidity ($p = 0.06$, $r = -0.17$), sample location in the furnace ($p = 0.04$, $r = 0.12$), and ambient barometric pressure ($p = 0.02$, $r = -0.19$). Importantly, we also found that several operational variables did not indicate a relationship with CNT forest characteristics: the storage of the samples in a desiccator (*versus* ambient), the ambient laboratory temperature, and the location on the source wafer from which the catalyst substrate was sampled.

Due to the duration (6 months) of the study, we considered whether or not to investigate the potential influence of catalyst age. However, prior studies on native oxide growth on Fe and Si surfaces indicate that, for nanoscale Fe layers, oxidation occurs in several nanoseconds upon exposure to oxygen at room temperature, and oxidation of clean Si wafer surfaces stabilizes after ~7 days under the same conditions.[27−30]

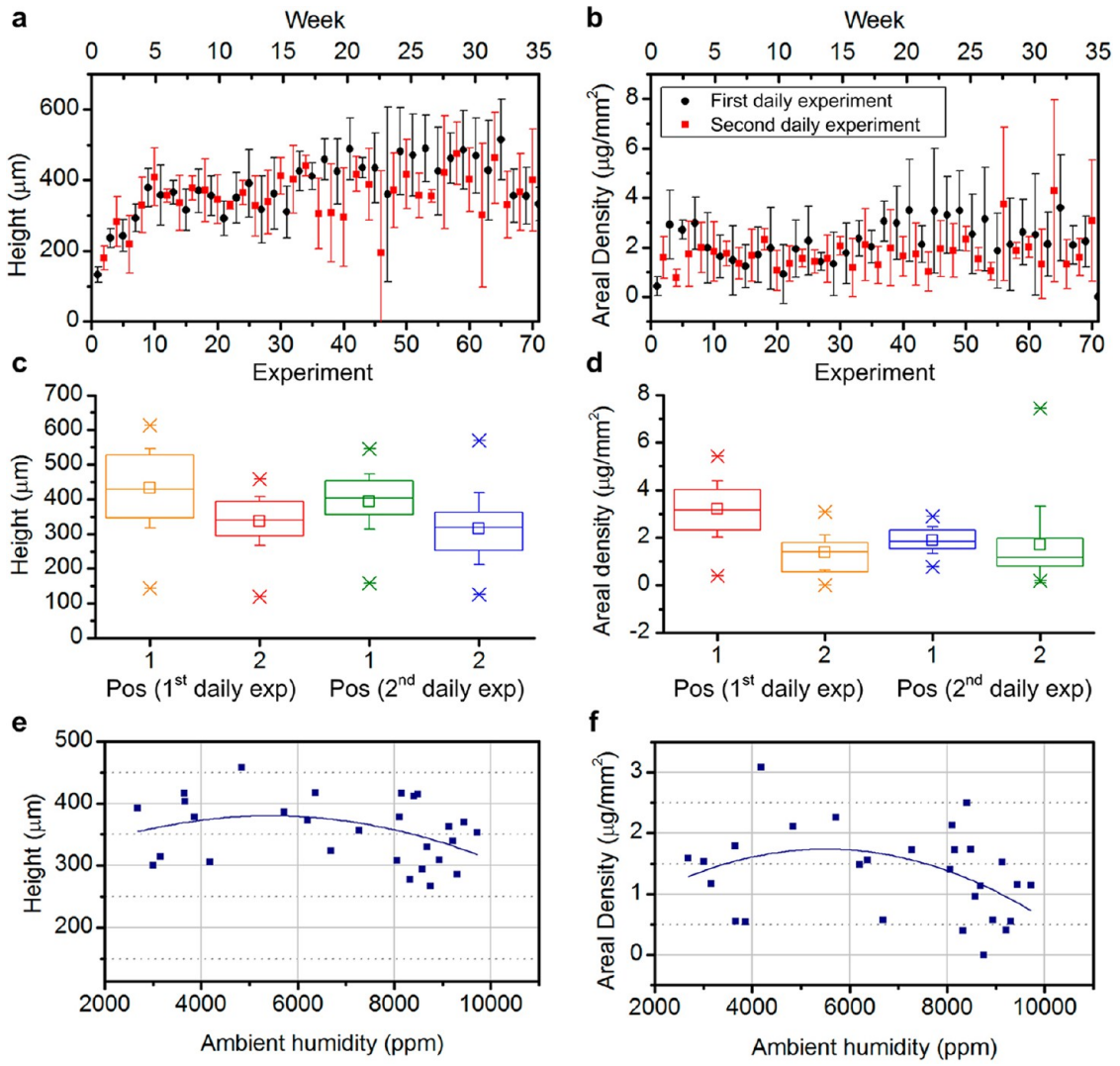

Figure 4. Initial analysis of reference growth variation, according to experiment order, sample placement, and measured ambient humidity. (a) Forest height *versus* experiment number, separated for the first and second experiment of each day. (b) Areal density *versus* experiment number. (c) Height data separated according to sample position in reactor and experiment order. (d) Areal density data separated according to sample position in reactor and experiment order. (e) Scatter plot of height *versus* ambient humidity for samples grown in position 2 and during the first experiment of the day, fitted with a polynomial relationship. (f) Scatter plot of areal density *versus* ambient humidity for samples grown in position 2 and during the first experiment of the day. In (e) and (f), the height values are the average of sample positions 2a and 2b. They show that an optimal value of ambient humidity maximizes either sample height or areal density.

Because the samples were stored in the lab ambient air for more than two weeks prior to the start of the study, it was assumed that the samples had reached a stable oxidation state.

All absolute *r*-values for significant variables fell in the range 0.10−0.30, indicating that each factor contributed to experimental variation, even if only subtly. This is in part due to the multivariate nature of the process; however, we later show that improving process control reduces growth variation significantly, thus reducing the size of the unknown parameter space and enabling future work to characterize individual variable-outcome correlations. Having identified major causes of variation, we now present a detailed analysis of each variable that we found contributes to variability.

Relationship between Ambient Humidity and Reactor Humidity. While we found that CNT forest height and areal density correlate with the ambient humidity in the laboratory, the humidity in the reactor tube is more relevant to the results of the growth experiment. Therefore, we had to determine the relationship between ambient humidity and reactor humidity. Additionally, because commercial hygrometers are sensitive to, and contaminated by, the hydrocarbons generated during CNT growth, we were not able to directly measure the moisture content in the hydrocarbon mixture exiting the furnace. Instead, we used the hygrometer to calibrate the H_2O ion current reading (AMU 18) from the quadrupole mass spectrometer. Calibration was performed using heated mixtures of H_2

TABLE 4. Calculated Correlation Coefficients between Selected Operational Variables and CNT Forest Height, Areal Density, and Volumetric Density[a]

	dependent variable *p*-value		
variable	forest height	areal density	volumetric density
sample location (1a, 1b, 2a, 2b)	**0.01**	**0.06**	0.20
desiccator (in/out)	0.49	0.73	0.88
wafer within batch (1, 2)	0.36	0.75	0.60
ambient humidity (ppm)	**0.00**	**0.04**	0.20
barometric pressure (Torr)	0.32	**0.02**	**0.00**

[a] Bold values represent statistically significant correlations.

and He/O_2, where H_2 and O_2 combined to form H_2O when heated above 550 °C.[31]

We found that the H_2O ion current measured by the mass spectrometer was directly related to the water content in ppm reported by the water vapor sensor, and we generated a linear correlation function. The correlation between ionization current (I) and reactor humidity (H) was derived from data gathered between 10 and 4000 ppm and is captured by the relationship

$$H = -490 + (1.84 \times 10^{14})I \quad (1)$$

The y-intercept of this equation is negative due to the finite baseline detection limit on the mass spectrometer. Applying this correlation function to the mass spectrometry data from the reference growth study enabled calculation of the reactor humidity during each experiment (Figure 5). This method of estimation verifies that there are significant fluctuations in the reactor humidity as well. However, we reiterate that this method of calculating reactor humidity is just an estimate but should be an ordinal indication of the humidity level within the reactor.

By this approach, we predict that the humidity within the reactor (mean steady-state value during the He purging step) was on average 15% of the ambient humidity in the laboratory during each corresponding experiment of the reference growth study. As shown in Figure 5b, the reactor humidity was highest during the anneal step of the first experiment of each day, after the tube was resting open to air for multiple days. With each progressive operation during the day (*i.e.*, first growth, second anneal, second growth, *etc.*) the reactor humidity decreased. As a result, the reactor humidity during any growth step was always less than that of the prior annealing step.

Throughout the study, the estimated average difference between the average reactor humidity during the first (1272 ppm) and second (570 ppm) experiment of the day was 702 ppm. By comparing these relative humidity levels in Figure 5, we concluded that performing a bake-out (see Methods) of the reactor immediately before an experiment reduces the amount of water vapor in the system by approximately 50% on average. However, even though the tube is baked after

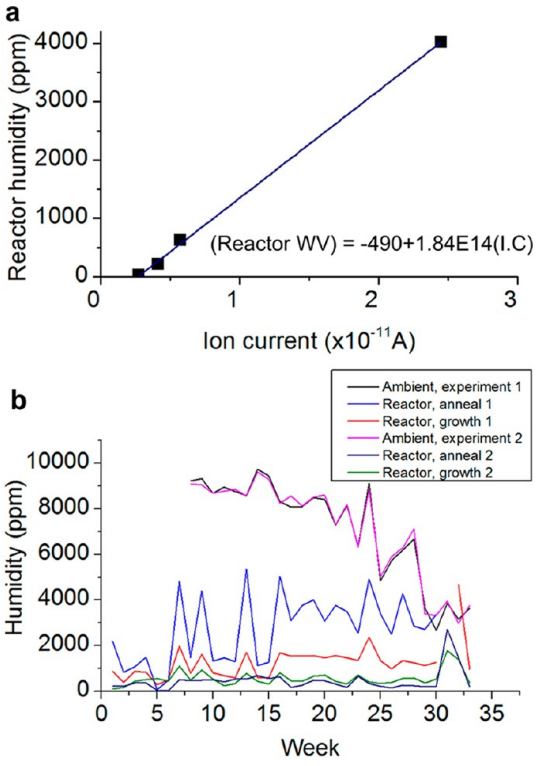

Figure 5. Measured relationship between ambient humidity and reactor humidity measured by mass spectrometry. (a) Linear relationship between reactor humidity and ionization current (AMU 18) of the mass spectrometer. (b) Comparison of ambient humidity and calculated reactor humidity during anneal and growth. Anneal and growth times are defined in Figure S5.

the first daily experiment, there is still a correlation between the humidity in the reactor during the second daily experiment and the ambient humidity in the lab. This suggested that some of the system components had a continuous influence on the reactor humidity level, as further indicated by decreasing moisture levels after subsequent bake-outs (Figure S3).

Reactor Tube Age and Gas Piping Material. To identify the means by which ambient lab humidity influences reactor humidity, we first investigated the influence of the age of the quartz reactor tube. A previous study suggested that the surface of the tube becomes coated with carbon over time, and this was shown to improve CNT forest growth.[11] We found that the inner surface of the quartz tube becomes more hydrophobic with age (Figure 6a inset), possibly due to graphitic deposits; however there is no change in adsorbed water vapor. We showed this in experiments (separate from the reference growth study) in which we dried two tubes—one that had been used for months of routine experiments, and another that was new—by flushing the tubes with ultrahigh-purity (UHP) He for 12 hours. We then let the tubes rest overnight in the lab ambient. Then, the tubes were each inserted into a reactor system that had been predried overnight using another tube and a 500 sccm flow of UHP He, which reached ~6 ppm H_2O

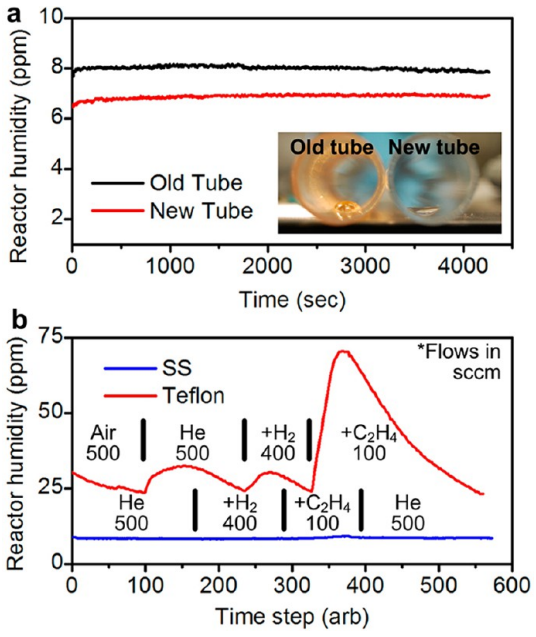

Figure 6. Effect of reactor tube age and gas delivery tube material on reactor humidity. (a) Moisture released from an old (>6 months) and new (<1 week) quartz tube upon heating. The tubes had been baked 12 h earlier. Inset picture shows that the contact angle of water on the interior of the quartz tube changes with age downstream of the sample. (b) Comparison of moisture vapor released from Teflon and stainless steel (SS) gas delivery, with all other conditions identical. All flows are in sccm.

as measured using the in-line hygrometer. Next, the furnace was heated to 750 °C with the same flow of 500 sccm of UHP He. As shown in Figure 6a, 1−2 ppm additional moisture was released by the old tube compared to the new tube.

This contrasted with our finding that significantly higher humidity levels are present in the CNT growth gases during a normal experiment. We next hypothesized that moisture was permeating the PTFE gas supply tubing and thereby becoming entrained in the gas mixture delivered to the CVD process. To quantify the moisture trapped in the gas flows, the reactor system was sealed with a dry quartz tube and left undisturbed (without any flow in the system) for 24 h, while 500 sccm of dry grade air was flowed through the hygrometer to keep moisture from collecting on the sensor. Then, the flow through the hygrometer was stopped and the hygrometer was opened to the furnace lines. While measuring the moisture at the output (without heating of the furnace), the gas flows were activated sequentially starting with 500 sccm He and later adding 400 sccm H_2 and then 100 sccm C_2H_4 after the hygrometer reading had stabilized at each flow.

As shown in Figure 6b, use of PTFE tubing (Swagelok, PFA-T4-062-100) to deliver the gases resulted in 10−50 ppm added moisture, with different values for each gas. The tubing was approximately 2 m long from the tank supply to each respective mass flow controller (MFC) and 1 m from the output of the MFCs (where the gases become mixed) to the input of the reactor. We repeated this experiment after replacing the PTFE tubing with stainless steel tubing (Swagelok, part no. SS-T4-S-035-20). Now, the measured moisture levels were less than 10 ppm, and negligible changes occurred when the different gases were introduced. Although these water vapor values seem low when compared to the values during the various growth experiments, it should be noted that the tubing experiments were conducted when ambient conditions were fairly dry. Summing the total ppm from each gas line and the tube (according to Figure 6a and b), we estimate a contribution of ~100 ppm. This value is one-third of the value measured for a "dry" day mass spectrometry reading during the first growth of the day. While this is a large difference, we argue that this error could still be due to the estimation of the ion current conversion to ppm (especially at lower ppm values). Further, based on the specifications for the gas cylinders (from PurityPlus), the H_2 tank should have <3 ppm H_2O and the He and C_2H_4 tanks should have <2 ppm H_2O. Gas cylinders of this purity have been used in previous work documenting CNT growth sensitivity studies.[32,33] Therefore, we concluded that permeability of the tubing was a major contribution to reactor humidity variation in our system.

Influence of Process Variation on Catalyst Morphology, CNT Diameter, and CNT Quality. Next, we quantified variations in alignment and diameter of CNTs within our forests using nondestructive small-angle X-ray scattering (SAXS). SAXS images were analyzed according to the procedure described by Wang *et al*. and Meshot *et al*.[34,35] Using a subset of samples, taken from experiments representative of the observed spread in ambient humidity, we determined correlations of alignment and diameter with process variables. The Hermans orientation parameter was calculated as a quantitative measure of CNT alignment, and the CNT diameter distribution was calculated by fitting a core−shell form factor model to line scans of the SAXS images. This procedure was previously verified to agree with TEM measurements of CNT diameter.[21]

As shown in Figure 7, we found that the mean CNT diameter increased with the ambient humidity. We also coupled CNT diameter with volumetric density of the CNT forests to calculate number density (number of CNTs per area), which showed an inverse relationship/correlation with ambient humidity. Because the thin-film catalyst was the same initial film thickness on each sample, a reduction of CNT number density is to be expected with an increase of average CNT diameter. This assumes that the volume of the catalyst thin film is conserved.

Previous studies suggest that moisture can influence the dewetting of catalyst thin films, the migration of catalyst atoms on the substrate,[36] and the lifetime of the catalyst during the growth process.[37] In order to determine the variables that govern the inverse

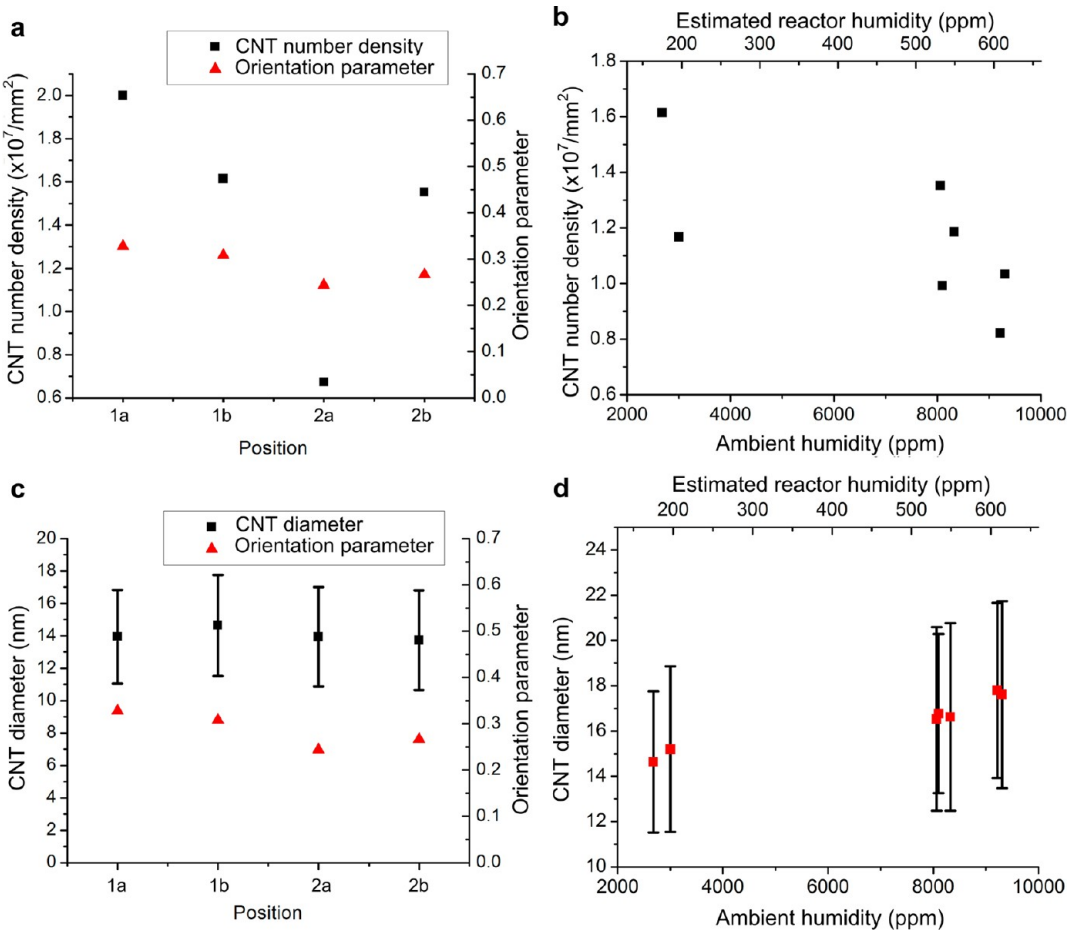

Figure 7. Impact of ambient humidity and substrate position on CNT diameter and number density. (a) Average CNT number density and Herman's orientation parameter *versus* substrate position on the boat. (b) CNT number density (average of all four samples) *versus* ambient humidity. (c) Average CNT diameter and Herman's orientation parameter *versus* substrate position on the boat. (d) Average CNT diameter *versus* ambient humidity.

relationship between CNT number density and reactor humidity, we focused on the annealing (dewetting) process, which determines the particle size and density on the substrate. Accordingly, we annealed catalyst substrate samples under controlled levels of reactor humidity. Guided by the reactor humidity derived from mass spectrometry for the reference growth experiments, three humidity levels were chosen: 37, 908, and 1668 ppm. Before preparing each sample, the CVD system (with stainless steel gas delivery tubing) was purged overnight to establish a baseline below 30 ppm H_2O. Then, in order to control the reactor humidity, a small amount of O_2 (*via* a mixture of 1% O_2 in He) was added to the nominal H_2/He gas flow used for annealing to generate H_2O, which we previously showed occurs when O_2 reacts with H_2 above 550 °C.[31] After the furnace temperature and humidity had stabilized, the substrate was moved to the heated zone, by translating the entire tube 25 cm so that the sample moved from outside the furnace to the standard growth location for sample positions 1a and 1b (Figure 1). Fifteen minutes after insertion, the sample was removed and cooled in the same gas atmosphere.

We note that, compared to the more frequent means of introducing moisture using a bubbler first shown by Hata *et al.*,[14] the He/O_2 method enables wide range control of the humidity level *via* conventional gas flow control hardware. However, residual O_2 is also present in the reactor due to incomplete conversion to H_2O.

Atomic force microscopy (AFM) characterization revealed a significant increase in catalyst particle diameter, height, and spacing with increasing reactor humidity. This trend is evident by inspection of the images in Figure 8, and we further analyzed particle spacing by applying a quantitative Voronoi-decomposition method to the images.[38] The relationship between particle spacing and reactor humidity is shown in Figure 9. This relationship explains why we observe larger CNT diameter and lower areal density with increasing humidity. Although we report merely an estimate of reactor humidity by eq 1, the trend of increasing particle size and spacing (Figure 8) with humidity is unequivocal, but may be affected by residual O_2 from the method used to generate H_2O for the samples. Even if this is the case, we conclude that the humidity range experienced during the

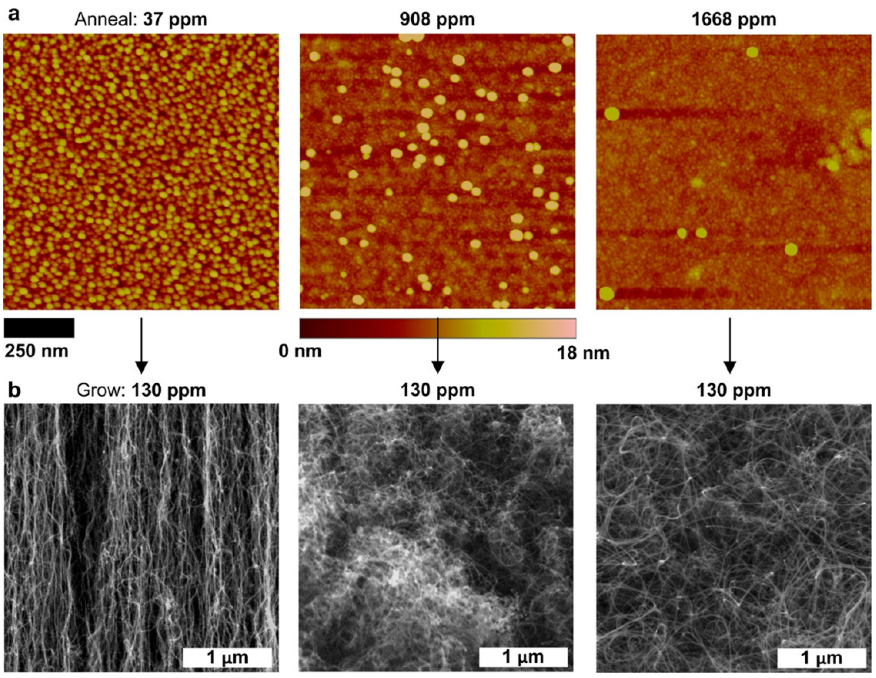

Figure 8. Effects of water content on catalyst particle size and density. (a) AFM images of catalyst films annealed in 37, 908, and 1668 ppm (left to right) H_2O. (b) SEM images of CNT morphology from the samples in (a). For (b) all samples were grown under identical conditions with 130 ppm H_2O measured at the outlet of the reactor before flowing C_2H_4 in the reactor.

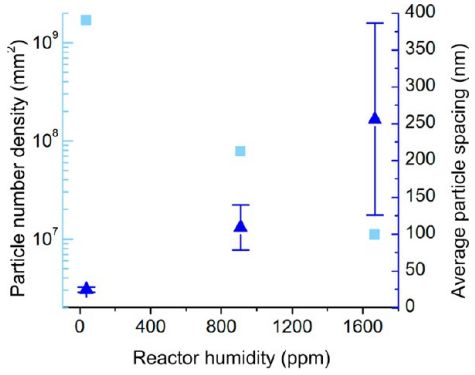

Figure 9. Measured relationship of both particle number density and average particle spacing (from AFM image analysis) with reactor humidity generated by adding He/O_2 to the reference annealing mixture of H_2/He.

reference growth study was broad enough to significantly change the catalyst morphology. The consequent effect on the CNT density is illustrated in Figure 8b, where CNTs are grown from the annealed samples in Figure 8a. As the humidity increases, the CNT morphology transitions from a vertically aligned forest to a tangled mat of CNTs caused by a decrease in the density of catalyst particles.

Nevertheless, important topics for future work include investigating how the humidity can influence the kinetics of activation and deactivation of catalyst Fe nanoparticles, which we have recently shown to be diameter dependent.[39] In addition, the role of Al_2O_3 and its interaction with H_2O during nucleation and growth, which may influence the catalyst stability and the ability of hydrocarbons to adsorb and possibly react on the oxide surface,[40,41] need to be studied further.

Last, the CNT quality was measured for 10 forests representing a range of ambient conditions using Raman spectroscopy. Raman spectroscopy was measured from the top surface of the forest so that both tall and short forests could be similarly compared (Figure S4). The G/D peak ratio, signifying structural quality of the CNTs, ranged from 1.12 to 1.88 with a median of 1.18. The majority (80%) of samples fell between 1.12 and 1.37, and no significant relationship was found between the G/D ratio and any of the documented variables. Because the Raman signature of MWNTs is generally weak compared to the strong resonant effect for SWNTs, we cannot conclude that the variations in reactor ambient influenced the quality of the CNTs within the forests. Although we did not find a systematic difference in CNT quality (by Raman spectroscopy), the presence of moisture may etch amorphous carbon depositions on the catalyst and/or the CNT walls.[14,37]

Sample Location in the Furnace Tube. It is known that sample position along the length of the quartz tube affects the height and uniformity of CNT forests and that there typically exists a "sweet spot" within the heated zone for CNT forest growth.[22,42] The sample position effect is caused by thermal history and the ensuing evolution of hydrocarbon chemistry along the length of the tube furnace. As the feedstock gas mixture of C_2H_4 and H_2 flows through the furnace, the thermal energy enables formation and recombination of myriad hydrocarbon species that can support

or hinder CNT growth. For instance, alkynes (triple-bonded carbon molecules) are important for efficient growth,[8,43,44] whereas much larger molecules, such as polycyclic aromatic hydrocarbons (PAHs), formed with increased thermal treatment, may either assist in productive growth pathways or promote soot formation.[44−46]

With this in mind, we found that the CNT forest height and density are also correlated to the sample position along the length of the quartz tube. We made this conclusion by comparing the mean height and density values from one sample position to every other position, using an ANOVA multiple comparison of means test. Specifically, the height in the upstream positions (1a, 1b) was on average 150 μm taller than in the downstream positions (2a, 2b), and areal density was greater by 0.75 μg/mm^2. Differences within the two side-by-side pairs were not significant (Figure S5). The temperature difference between sample positions 1 and 2 was <15 °C. Also, SAXS analysis confirmed that CNT diameter and alignment did not vary according to the sample position, indicating that the height and density correlation with position was due to local gas composition during growth.

We conclude that the composition of the feedstock gases arising from thermal treatment in the reactor is the main source of the sample position effect in our study, although a previous study has suggested that reactive gases generated by the catalyst on the upstream samples can influence growth on the downstream samples.[33] To further support this point, we conducted experiments where single samples were placed at positions 1 and 2 for separate growth runs and found that the upstream samples were approximately 260 μm taller than the downstream samples.

Moreover, by analysis of the full data set (Figure 4c,d) we found that a larger portion of the variability in height and density was from sample position in the reactor (*i.e.*, experiments from the same relative time of the day over multiple days) than from ambient factors (*i.e.*, the differences in consecutive (nominally identical) experiments). Thus, there is a need for strict control of sample position within tube furnace systems or development and evaluation of systems that generate spatially more uniform temperature and gas conditions, in addition to controlling ambient exposure.

Barometric Pressure. We also found that ambient pressure can influence CNT growth results. Stadermann and colleagues reported that CNT forest height is sensitive to the reactor pressure and that precise control of pressure, in concert with controlled introduction of water vapor (1500 ppm), improves process consistency.[9] In our system, ambient pressure is communicated to the reactor tube *via* the exhaust bubbler, and thus, a change in pressure downstream of the bubbler changes the pressure inside the tube. We verified this using an inline pressure transducer. The volume of the oil inside the bubbler can also affect the pressure, but this was kept constant throughout the study.

During the reference growth study, we measured ambient pressure averaging 766 Torr with a standard deviation of 8 Torr. Within a range of 740−780 Torr, we found an inverse relationship ($r = -0.19$) between ambient pressure and CNT forest density; therefore, higher density forests were produced on average at lower pressure, and more importantly precise control of reactor pressure is important to achieve highly consistent results. We hypothesize that such slight pressure fluctuations influence the partial pressures of the complex hydrocarbon mixture that evolves thermally with flow through the reactor. This is one aspect of Le Chatelier's principle: when the system is exposed to an increase in total pressure, the volume of the reactants changes, resulting in a shift of the equilibrium of the reaction. Thus, improved control of reactor pressure will stabilize the reaction over multiple runs.

Analysis of Patterned CNT Forests. Growth of CNT microstructures from lithographically patterned catalyst substrates was carried out on the same day as the corresponding nonpatterned experiments, but occurred at least 8 h later to allow for interactions between the ambient conditions and the reactor system to take place and thereby "reset" the system. The same pattern was used for each experiment, and the pattern had arrays of microstructures with diameter ranging from 160 to 320 μm and varying cross-section from a thin annulus (2 μm wall thickness) to a solid circle. We considered the average microstructure height and the number of defects (*e.g.*, missing or deformed microstructures) to be measures of the quality of CNT microstructure growth. Selected sample growths are shown in Figure 10, corresponding to the upstream position during the first daily experiment.

While the number of defects was lower in position 1, we did not find a statistical correlation between CNT microstructure height and ambient humidity, even though we found a correlation for forest height. We theorize this is due to spacing between catalyst patterns and the affect this proximity has on localized gas atmosphere. However, variation in height was significant, where the coefficient of variation was 19%, although lower than the value of 31% observed for nonpatterned forests. The defects were mostly observed for patterns with small wall thicknesses, becoming more pronounced during experiments 38 to 58, which correspond to the large fluctuations in ambient humidity.

Qualitatively, the most extreme variation was also noticed on the thin-walled features, which in some cases did not grow CNT forests and in other cases were considerably deformed, presumably due to a lower

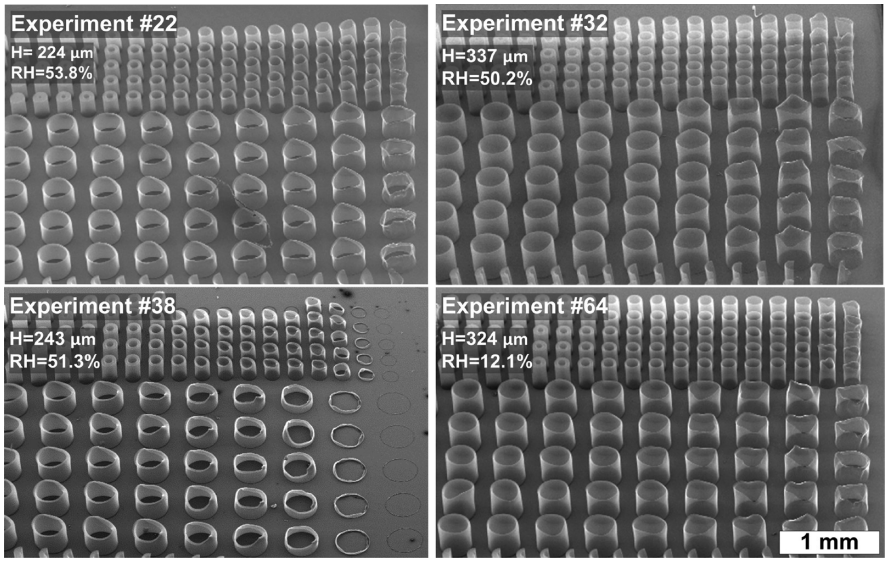

Figure 10. Images representing variation of CNT microstructure growth from patterned catalyst films, processed identically with the nonpatterned substrates for the reference growth study. The experiment numbers correspond to the same date as the run number for forest growth, and the relative humidity was measured as described in the Methods.

CNT packing density. Further analysis of patterned growth is beyond the scope of this study; however, our findings suggest that additional factors, beyond those that we systematically addressed, are responsible for variation in patterned CNT growth. These include the size and spacing of the features,[47] which, by interaction of the catalyst with the gas mixture, could result in chemical coupling between adjacent microstructures. There may also be a relationship between total catalyst area and ambient conditions, meaning that different optimal conditions would be needed to maximize consistency of patterned *versus* nonpatterned CNT forests.

System Modifications and Process Improvement. Guided by the results of the reference growth study and follow-up experiments, we made several modifications to our CVD system, designed to reduce sensitivity to ambient fluctuations while maintaining flexibility in configuration and operation. These modifications were made after the conclusion of the reference growth study and during investigation of the factors that contributed to variation. Specifically we installed a hygrometer (Cermet II) upstream of the furnace to monitor system water content, replaced the PTFE gas delivery lines with stainless steel lines to limit the transfer of water into the system from the surrounding lab environment, and implemented a continuous purge of He (100 sccm, UHP grade) to keep the system clean and dry when not in use for CNT growth. Moreover, we designed and built a new automated CVD system to interface with a standard tube furnace. This system automatically loads and unloads the furnace using a motorized arm and a load lock that houses several catalyst substrates for sequential CNT growth. The design and testing of this custom system will be presented in a subsequent publication.[48]

Using the automated system along with the reference growth procedure, a significant reduction in statistical variation in CNT height and density was realized. We performed a smaller-scale study, involving 26 growth experiments over 12 weeks, using 2 samples per experiment. The samples were placed at positions equivalent to (1a, 1b) from the reference growth study. The automated system resulted in decreased variation of both CNT forest height and density by 50% and 54%, respectively (Figure 11). During this series, the reactor humidity varied from 100 to 150 ppm (Figure 11b), compared to 100−2000 ppm (Figures 5b, S6) for the first daily experiment during the reference growth study. This demonstrates the importance of a consistent lab procedure and the significant improvement in results that can be achieved by standardization of the process, including limiting reactor exposure to the ambient conditions during sample loading through constant purging of dry gases when the reactor is open.

However, the data from our improved process still show variation, specifically a coefficient of variation of 15% (mean = 584 ± 87 μm) for CNT forest height and 25% (mean = 6 ± 1.5 μg/mm^2) for areal density. Despite the remaining variation, it is certain that humidity control is beneficial and contributing to this reduced variation. However, because there is no longer a correlation between ambient humidity and height or density, other factors may be responsible for the remaining variation, and it may be necessary now to tune the reactor humidity level according to the other process parameters (gas mixture, temperature, catalyst) in order to optimize CNT forest characteristics.

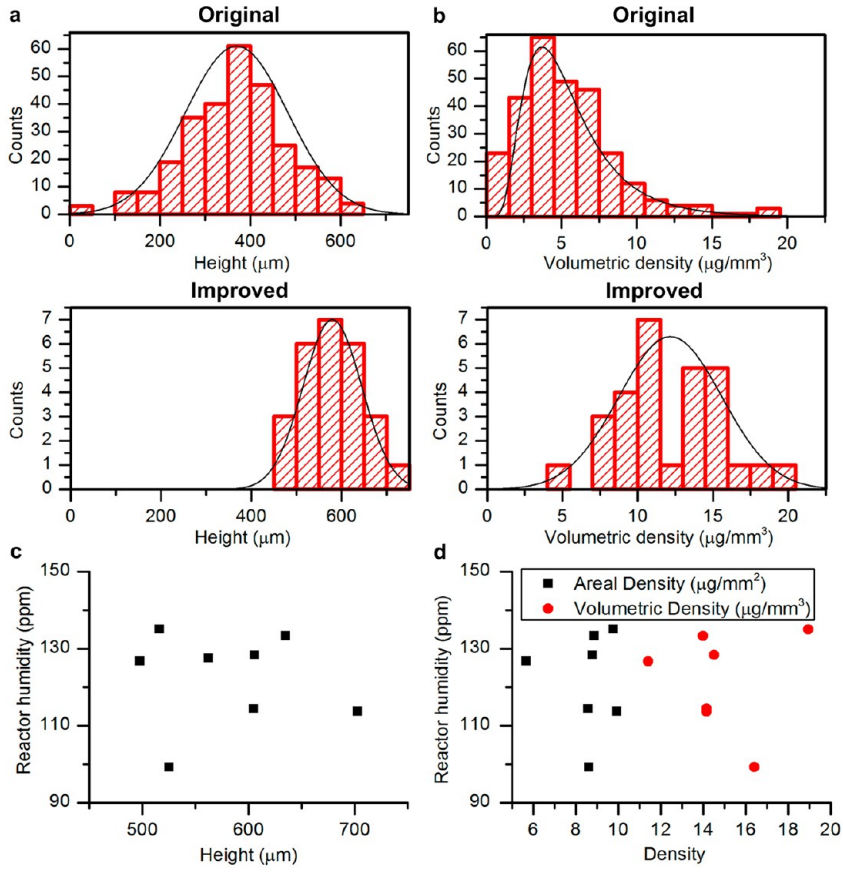

Figure 11. Reduced variation in CNT forest growth *via* improvement of process consistency. (a, b) Histograms of height and volumetric density before and after implementing the modifications discussed in the text. (c, d) Scatter plots corresponding to the histograms, relating height and density to reactor humidity for the improved process. Due to limited availability of the hygrometer during this portion of the study, only 8 samples have reactor humidity data shown in (c, d).

Additionally, to discover the remaining contributions to growth variation, further study is needed of other contaminants (*e.g.*, oxygen) in the reactant mixture, the influence of inherent moisture changes during both annealing and growth, the influence of reactor pressure, the accuracy and repeatability of gas flow control, and potential trace metal contaminants in the thin-film catalyst.

Last, we summarize a list of recommended control practices, which, in addition to the synthesis recipe, will reduce variability in CNT growth outcomes particularly when operating in a normal lab environment.

- Continuous purging of the system under a slow flow of inert gas (*e.g.*, 100 sccm He) or dry air to control moisture level while at rest
- Use of stainless steel tubing throughout the system rather than polymer (*e.g.*, Tygon or PTFE) tubing, except for the quartz reaction tube
- Use of a single quartz tube for all experiments that involve the same materials for the substrate and catalyst. Use dedicated quartz tubes for each different set of materials or significantly different process conditions (*e.g.*, gas mixture, temperature range).
- Baking of the quartz tube and boat with a flow of air after every growth experiment, for at least 10 min at a temperature equal to or greater than the CNT growth temperature
- Consistent placement of the sample, with *ca.* millimeter repeatability with respect to the position of the furnace thermocouple
- Calibration of all mass flow controllers, such as using a bubble flow meter, at intervals recommended by the manufacturer
- Measurement of the deposited catalyst thickness using AFM, and calibration of thin-film deposition crystal gauges accordingly

Complementary to these recommendations, a detailed video procedure for CNT forest growth from micropatterned catalysts has been published by Copic *et al.*[49] This shows our methods for loading and unloading the reactor before and after the CNT growth process and provides a visual description of the catalyst preparation method and the CVD system.

CONCLUSIONS

We demonstrated that a standardized CNT forest growth procedure can be used to identify primary sources of CNT growth variation using a standard

atmospheric pressure CVD system and silicon substrate samples with a thin-film catalyst. Statistical analysis of 280 samples resulting from 70 experiments over a 6-month period showed that ambient humidity, barometric pressure, and sample position in the CVD furnace contribute significantly to experiment-to-experiment variation. Quantitative characterization of the catalyst particle size and spacing from samples processed at different controlled in-reactor humidity levels showed that humidity influences the dewetting and annealing of the catalyst film. This was directly related to the CNT diameter and spacing. Moreover, consistent placement of the samples within the furnace is required due to evolution of the reactant mixture with continued treatment. These and other outcomes allowed us to implement several changes to the CVD system and lab practices, such as replacing sections of PTFE gas delivery tubing. These changes reduced uncontrolled run-to-run variation in CNT forest height and density by more than 50%. We hope that increased adoption of standard growth practices and statistical analyses will accelerate progress in reproducible CNT synthesis to accelerate laboratory research and application-focused materials development.

METHODS

Substrate Preparation. Two (100) silicon wafers (with 300 nm of thermally grown SiO_2) were first coated with photoresist on both sides and then scored using a dicing saw (ADT 7100) to create 5 × 5 mm square lines on the back of the wafers, 50 μm deep. The photoresist was then removed from both sides of the wafers, and then 10 nm of Al_2O_3, followed by 3 nm of Fe, was deposited by e-beam evaporation (SJ-26). The deposition produced two wafers that were used for the entire study. Afterward, each 5 × 5 mm square was marked with a unique identifying number so we could track the location it came from on the wafer as well as orient the sample in the same direction on the boat.

CVD System. The system was composed of the following main sections: gas delivery, reactor/furnace, and mass spectrometer. Ultrapure (99.99%) H_2, He, and C_2H_4 gases were controllably delivered using MFCs (Omega and Aalborg, model GFC17) to a Lindberg Blue M horizontal tube furnace (25 mm o.d., 300 mm heated length). Zero grade dry air for the system bake-out between growths was metered *via* a manual flow meter (McMaster-Carr, model 5079K63). Finally, the mass spectrometer (Pfeiffer Vacuum Technology, model GSD301O3) was connected downstream of the furnace in the exhaust line to analyze gas species variation from experiment to experiment and measure in-tube water content.

Instrument Calibration. The deposition thickness produced by the e-beam deposition machine was calibrated the week before the sample wafers were generated by AFM measurements of deposited thin films on other samples. AFM imaging was performed in tapping mode in a Veeco Dimension Icon. The calibration of the laser displacement sensor used to measure CNT forest height was verified *via* a gauge block (Mitutoyo 080076) before each set of height measurements. An MFC configured to be a mass flow meter (Aalborg model GFC17) was used in-line with the CVD system MFCs to calibrate the flow rates at four equally spaced points between 0 sccm and the maximum flow of the MFC to be calibrated (1000 sccm for He, 100 sccm for C_2H_4, and 1000 sccm for H_2). Each MFC was calibrated before the beginning of the study and verified at the end of the study to account for any drift in the system. A temperature profile of the Lindberg furnace was taken using a K-type thermocouple with the furnace at 775 °C every centimeter along its long axis. This was measured at the beginning and again at the end of the study to ensure the furnace temperature had not drifted (it was also used to calibrate the built-in thermocouple of the furnace). In addition, a log of gas tank replacement was kept to rule out the effect of tank contamination in this study.

Reference Growth Procedure. Random samples from the wafer depositions were selected and placed in the etched wells (250 μm deep) of the boat. The boat was then loaded into the quartz tube (22 mm i.d. × 762 mm long), and its upstream edge placed 40 mm downstream of the center of the furnace. VACNT arrays were grown at atmospheric pressure, with flows of 100/100/400 sccm C_2H_4/H_2/He, at 775 °C for 10 min, preceded by an annealing step at 775 °C for 10 min with flows of 100/400 sccm H_2/He. The CNTs were rapidly cooled in a He atmosphere until the chamber temperature reached 150 °C, at which point the samples were removed. After sample removal, the boat was loaded back into the quartz tube, and both the boat and the tube were baked with air (500 sccm) for 30 min at 875 °C. Ambient conditions in the lab (temperature and relative humidity), during CNT synthesis, were collected by a USB ambient monitor (UEi, model THL1).

Characterization. The length and width of each sample were measured using calipers and used to calculate the sample area. A laser displacement sensor (Keyence, model LK-G152) was used to measure the height of the CNT forest where the sample was placed on a flat stage and covered with a chosen piece of Si 500 μm thick. The laser measured the height at five locations (four corners and center), three times each, to estimate the average height of the forest (determined after subtracting the thickness of the Si substrate and cover plate). Mass measurements of the substrates were collected before and after CNT growth, using a microbalance (Ohaus Discovery), and the differential represented the mass of CNTs grown on the substrate. The combination of the mass, area, and height measurements was used to calculate the areal and volumetric densities of the VACNT arrays. CNT structural quality was evaluated by Raman analysis (Dimension P2, Lambda Solutions, λ = 533 nm) from the top of the forest. Sidewalls were not measured due to the height of the forest. Quality of the forest was assessed using the ratio of the I_G and I_D peak. SEM imaging was performed using a FEI Nova Nanolab.

For X-ray scattering measurements, the CNT forest is placed on a motorized stage in the beampath of the G1 beamline at Cornell High Energy Synchrotron Source (CHESS). A beam energy of 10 (0.1 keV (wavelength ≈ 0.13 nm)) is selected with synthetic multilayer optics (W/B4C, 27.1 Å *d*-spacing), and the beam is focused down to ~20 μm using mechanical slits upstream. The beam size is accurately measured by scanning the beam over a pinhole slit mounted on a motorized stage while measuring the beam intensity. The downstream X-ray intensity measurements are normalized to the upstream measurements in order to eliminate the effect of the drift in synchrotron intensity with time. A standard sample of silver behenate powder (d_{001} = 58.380 Å) is used to calibrate the pixel-to-*q* ratio. Line scans from the 2D SAXS patterns are fitted using a mathematical model for log-normally distributed hollow cylinders. These scans are obtained by integration of intensities within ±10° from the reference direction (*x*-axis) of the inverse space parameter *q* (chosen to be the direction of maximum intensity). The fitting code used an iterative approach in searching for the best fit within a user-defined fitting range. By including the low-*q* part of the data, a good fit was achieved that selects a probability density function (PDF) for diameter distribution as well as for the ratio *c* = i.d./o.d., where i.d. is the inner diameter of the CNT and o.d. is the outer diameter.

Conflict of Interest: The authors declare no competing financial interest.

Supporting Information Available: Additional data and figures as described in the text. This material is available free of charge *via* the Internet at http://pubs.acs.org.

Acknowledgment. We thank A. Woll for assistance with X-ray scattering instrument setup and data collection. We also thank D. Copic for assistance with Raman spectroscopy; Jinjing Li for SEM imaging of patterned CNT growth; and D. Plata for helpful discussions regarding the influence of hydrocarbon chemistry and moisture on CNT growth. Financial support was provided by the Scalable Nanomanufacturing Program of the National Science Foundation (DMR-1120187), the Office of Naval Research (N000141010556), and the University of Michigan *via* startup funds to A.J.H. C.R.O. was supported in part by a University of Michigan Mechanical Engineering Department Fellowship. E.S.P. acknowledges the DoD, Air Force Office of Scientific Research, National Defense Science and Engineering Graduate (NDSEG) Fellowship, 32 CFR 168a. X-ray scattering was performed in the G1 beamline at the Cornell High-Energy Synchrotron Source (CHESS), which is supported by the NSF and the National Institutes of Health under Grant DMR-0225180. Electron microscopy and AFM were performed at the University of Michigan Electron Microbeam Analysis Library (EMAL), and microfabrication was performed at the Lurie Nanofabrication Facility (LNF), which is a member of the National Nanotechnology Infrastructure Network (NNIN).

REFERENCES AND NOTES

1. Roco, M. C.; Mirkin, C. A.; Hersam, M. C. *Nanotechnol. Res. Directions Soc. Needs 2020*; Springer: Berlin, 2010; pp 1−610.
2. Huang, H.; Liu, C. H.; Wu, Y.; Fan, S. Aligned Carbon Nanotube Composite Films for Thermal Management. *Adv. Mater.* **2005**, *17*, 1652–1656.
3. Marconnet, A. M.; Yamamoto, N.; Panzer, M. A.; Wardle, B. L.; Goodson, K. E. Thermal Conduction in Aligned Carbon Nanotube-Polymer Nanocomposites with High Packing Density. *ACS Nano* **2011**, *5*, 4818–4825.
4. Tong, T.; Zhao, Y.; Delzeit, L.; Kashani, A.; Meyyappan, M.; Majumdar, A. Dense Vertically Aligned Multiwalled Carbon Nanotube Arrays as Thermal Interface Materials. *IEEE Trans. Compon. Packag. Technol.* **2007**, *30*, 92–100.
5. Esconjauregui, S.; Fouquet, M.; Bayer, B. C.; Ducati, C.; Smajda, R.; Hofmann, S.; Robertson, J. Growth of Ultrahigh Density Vertically Aligned Carbon Nanotube Forests for Interconnects. *ACS Nano* **2010**, *4*, 7431–7436.
6. Fu, W.; Liu, L.; Jiang, K.; Li, Q.; Fan, S. Super-Aligned Carbon Nanotube Films as Aligning Layers and Transparent Electrodes for Liquid Crystal Displays. *Carbon* **2010**, *48*, 1876–1879.
7. Tawfick, S.; O'Brien, K.; Hart, A. J. Flexible High-Conductivity Carbon-Nanotube Interconnects Made by Rolling and Printing. *Small* **2009**, *5*, 2467–2473.
8. Plata, D.; Meshot, E.; Reddy, C. Multiple Alkynes React with Ethylene to Enhance Carbon Nanotube Synthesis, Suggesting a Polymerization-Like Formation Mechanism. *ACS Nano* **2010**, *4*, 7185–7192.
9. Stadermann, M.; Sherlock, S. P.; In, J.-B.; Fornasiero, F.; Park, H. G.; Artyukhin, A. B.; Wang, Y.; Yoreo, J. J. De; Grigoropoulos, C. P.; Bakajin, O.; *et al*. Mechanism and Kinetics of Growth Termination in Controlled Chemical Vapor Deposition Growth of Multiwall Carbon Nanotube Arrays. *Nano Lett.* **2009**, *9*, 738–744.
10. Futaba, D.; Hata, K.; Yamada, T.; Mizuno, K.; Yumura, M.; Iijima, S. Kinetics of Water-Assisted Single-Walled Carbon Nanotube Synthesis Revealed by a Time-Evolution Analysis. *Phys. Rev. Lett.* **2005**, *95*, 056104(1)–056101(4).
11. Liu, K.; Liu, P.; Jiang, K.; Fan, S. Effect of Carbon Deposits on the Reactor Wall during the Growth of Multi-Walled Carbon Nanotube Arrays. *Carbon* **2007**, *45*, 2379–2387.
12. Terranova, M. L.; Sessa, V.; Rossi, M. The World of Carbon Nanotubes: An Overview of CVD Growth Methodologies. *Chem. Vap. Deposition* **2006**, *12*, 315–325.
13. Nessim, G. D. Properties, Synthesis, and Growth Mechanisms of Carbon Nanotubes with Special Focus on Thermal Chemical Vapor Deposition. *Nanoscale* **2010**, *2*, 1306–1323.
14. Hata, K.; Futaba, D. N.; Mizuno, K.; Namai, T.; Yumura, M.; Iijima, S. Water-Assisted Highly Efficient Synthesis of Impurity-Free Single-Walled Carbon Nanotubes. *Science* **2004**, *306*, 1362–1364.
15. Deepak, F. L.; Govindaraj, a.; Rao, C. N. R. Improved Synthesis of Carbon Nanotubes with Junctions and of Single-Walled Carbon Nanotubes. *J. Chem. Sci.* **2006**, *118*, 9–14.
16. Cao, A.; Zhang, X.; Xu, C.; Liang, J.; Wu, D.; Wei, B. Aligned Carbon Nanotube Growth under Oxidative Ambient. *J. Mater. Res.* **2011**, *16*, 3107–3110.
17. Zhang, G.; Mann, D.; Zhang, L.; Javey, A.; Li, Y.; Yenilmez, E.; Wang, Q.; McVittie, J. P.; Nishi, Y.; Gibbons, J.; *et al*. Ultra-High-Yield Growth of Vertical Single-Walled Carbon Nanotubes: Hidden Roles of Hydrogen and Oxygen. *Proc. Natl. Acad. Sci. U.S.A.* **2005**, *102*, 16141–16145.
18. Futaba, D. N.; Goto, J.; Yasuda, S.; Yamada, T.; Yumura, M.; Hata, K. General Rules Governing the Highly Efficient Growth of Carbon Nanotubes. *Adv. Mater.* **2009**, *21*, 4811–4815.
19. Plata, D. L.; Hart, A. J.; Reddy, C. M.; Gschwend, P. M. Early Evaluation of Potential Environmental Impacts of Carbon Nanotube Synthesis by Chemical Vapor Deposition. *Environ. Sci. Technol.* **2009**, *43*, 8367–8373.
20. Meshot, E. R.; Plata, D. L.; Tawfick, S.; Zhang, Y.; Verploegen, E. A.; Hart, A. J. Engineering Vertically Aligned Carbon Nanotube Growth by Decoupled Thermal Treatment of Precursor and Catalyst. *ACS Nano* **2009**, *3*, 2477–2486.
21. Bedewy, M.; Meshot, E. R.; Reinker, M. J.; Hart, A. J. Population Growth Dynamics of Carbon Nanotubes. *ACS Nano* **2011**, *5*, 8974–8989.
22. Hart, A. J.; Slocum, A. H. Rapid Growth and Flow-Mediated Nucleation of Millimeter-Scale Aligned Carbon Nanotube Structures from a Thin-Film Catalyst. *J. Phys. Chem. B* **2006**, *110*, 8250–8257.
23. Bedewy, M.; Meshot, E. R.; Guo, H.; Verploegen, E. A.; Lu, W.; Hart, A. J. Collective Mechanism for the Evolution and Self-Termination of Vertically Aligned Carbon Nanotube Growth. *J. Phys. Chem. C* **2009**, *113*, 20576–20582.
24. Chakrabarti, S.; Nagasaka, T.; Yoshikawa, Y.; Pan, L.; Nakayama, Y. Growth of Super Long Aligned Brush-Like Carbon Nanotubes. *Jpn. J. Appl. Phys.* **2006**, *45*, L720–L722.
25. Nessim, G. D.; Hart, A. J.; Kim, J. S.; Acquaviva, D.; Oh, J.; Morgan, C. D.; Seita, M.; Leib, J. S.; Thompson, C. V. Tuning of Vertically-Aligned Carbon Nanotube Diameter and Areal Density through Catalyst Pre-Treatment. *Nano Lett.* **2008**, *8*, 3587–3593.
26. Raudenbush, S. W.; Liu, W.; Martinez, A.; Spybrook, J. *Optimal Design Software for Multi-Level and Longitudinal Research* (Version 3.01) [Software], 2011. Available from www.wtgrantfoundation.org.
27. Jeon, B.; Van Overmeere, Q.; van Duin, A. C. T.; Ramanathan, S. Nanoscale Oxidation and Complex Oxide Growth on Single Crystal Iron Surfaces and External Electric Field Effects. *Phys. Chem. Chem. Phys. (PCCP)* **2013**, *15*, 1821–1830.
28. Stumm, W.; Lee, G. F. Oxygenation of Ferrous Iron. *Ind. Eng. Chem.* **1961**, *53*, 143–146.
29. Leibbrandt, G. W. R.; Hoogers, G.; Habraken, F. H. P. M. Thin Oxide Film Growth on Fe(100). *Phys. Rev. Lett.* **1992**, *68*, 1947–1950.
30. Morita, M.; Ohmi, T.; Hasegawa, E.; Kawakami, M.; Ohwada, M. Growth of Native Oxide on a Silicon Surface. *J. Appl. Phys.* **1990**, *68*, 1272–1281.
31. Nessim, G. D.; Al-Obeidi, A.; Grisaru, H.; Polsen, E. S.; Oliver, C. R.; Zimrin, T.; Hart, A. J.; Aurbach, D.; Thompson, C. V. Synthesis of Tall Carpets of Vertically Aligned Carbon Nanotubes by *in-Situ* Generation of Water Vapor through Preheating of Added Oxygen. *Carbon* **2012**, *50*, 4002–4009.
32. In, J. B.; Grigoropoulos, C. P.; Chernov, A. A.; Noy, A. Hidden Role of Trace Gas Impurities in Chemical Vapor Deposition Growth of Vertically-Aligned Carbon Nanotube Arrays. *Appl. Phys. Lett.* **2011**, *98*, 153102(1)–153102(3).
33. In, J. B.; Grigoropoulos, C. P.; Chernov, A. A.; Noy, A. Growth Kinetics of Vertically Aligned Carbon Nanotube Arrays in Clean Oxygen-Free Conditions. *ACS Nano* **2011**, *5*, 9602–9610.

34. Wang, B. N.; Bennett, R. D.; Verploegen, E.; Hart, A. J.; Cohen, R. E. Quantitative Characterization of the Morphology of Multiwall Carbon Nanotube Films by Small-Angle X-ray Scattering. *J. Phys. Chem. C* **2007**, *111*, 5859–5865.
35. Meshot, E. R.; Hart, A. J. Abrupt Self-Termination of Vertically Aligned Carbon Nanotube Growth. *Appl. Phys. Lett.* **2008**, *92*, 113107(1)–113107(3).
36. Amama, P. B.; Pint, C. L.; McJilton, L.; Kim, S. M.; Stach, E. A.; Murray, P. T.; Hauge, R. H.; Maruyama, B. Role of Water in Super Growth of Single-Walled Carbon Nanotube Carpets. *Nano Lett.* **2009**, *9*, 44–49.
37. Yamada, T.; Maigne, A.; Yudasaka, M.; Mizuno, K.; Futaba, D. N.; Yumura, M.; Iijima, S.; Hata, K. Revealing the Secret of Water-Assisted Carbon Nanotube Synthesis by Microscopic Observation of the Interaction of Water on the Catalysts. *Nano Lett.* **2008**, *8*, 4288–4292.
38. Meshot, E. R.; Verploegen, E.; Bedewy, M.; Tawfick, S.; Woll, A. R.; Green, K. S.; Hromalik, M.; Koerner, L. J.; Philipp, H. T.; Tate, M. W.; *et al*. High-Speed *in-Situ* X-ray Scattering of Carbon Nanotube Film Nucleation and Self-Organization. *ACS Nano* **2012**, *6*, 5091–5101.
39. Bedewy, M.; Meshot, E. R.; Hart, a. J. Diameter-Dependent Kinetics of Activation and Deactivation in Carbon Nanotube Population Growth. *Carbon* **2012**, *50*, 5106–5116.
40. Magrez, A.; Smajda, R.; Seo, J. W.; Horváth, E.; Ribic, P. R.; Andresen, J. C.; Acquaviva, D.; Olariu, A.; Laurenczy, G.; Forró, L. Striking Influence of the Catalyst Support and Its Acid-Base Properties: New Insight into the Growth Mechanism of Carbon Nanotubes. *ACS Nano* **2011**, *5*, 3428–3437.
41. Wischert, R.; Laurent, P.; Copéret, C.; Delbecq, F.; Sautet, P. γ-Alumina: The Essential and Unexpected Role of Water for the Structure, Stability, and Reactivity of "Defect" Sites. *J. Am. Chem. Soc.* **2012**, *134*, 14430–14449.
42. Li, G.; Chakrabarti, S.; Schulz, M.; Shanov, V. The Effect of Substrate Positions in Chemical Vapor Deposition Reactor on the Growth of Carbon Nanotube Arrays. *Carbon* **2010**, *48*, 2111–2115.
43. Zhong, G.; Hofmann, S.; Yan, F.; Telg, H.; Warner, J. H.; Eder, D.; Thomsen, C.; Milne, W. I.; Robertson, J. Acetylene: A Key Growth Precursor for Single-Walled Carbon Nanotube Forests. *J. Phys. Chem. C* **2009**, *113*, 17321–17325.
44. Eres, G.; Kinkhabwala, A. a; Cui, H.; Geohegan, D. B.; Puretzky, A. A.; Lowndes, D. H. Molecular Beam-Controlled Nucleation and Growth of Vertically Aligned Single-Wall Carbon Nanotube Arrays. *J. Phys. Chem. B* **2005**, *109*, 16684–16694.
45. Nessim, G. D.; Seita, M.; Plata, D. L.; O'Brien, K. P.; Hart, A. J.; Meshot, E. R.; Reddy, C. M.; Gschwend, P. M.; Thompson, C. V. Precursor Gas Chemistry Determines the Crystallinity of Carbon Nanotubes Synthesized at Low Temperature. *Carbon* **2011**, *49*, 804–810.
46. Richter, H.; Howard, J. Formation of Polycyclic Aromatic Hydrocarbons and Their Growth to Soot—A Review of Chemical Reaction Pathways. *Prog. Energy Combust. Sci.* **2000**, *26*, 565–608.
47. Jeong, G.-H.; Olofsson, N.; Falk, L. K. L.; Campbell, E. E. B. Effect of Catalyst Pattern Geometry on the Growth of Vertically Aligned Carbon Nanotube Arrays. *Carbon* **2009**, *47*, 696–704.
48. Oliver, C. R.; Westrick, W.; Koehler, J.; Cruz-Gonzalez, T.; Brieland-Shoultz, A.; Hart, A. J. Robofurnace: Automated CVD for High-Throughput Research and Process Optimization/Discovery (in preparation).
49. Copic, D.; Park, S. J.; Tawfick, S.; Volder, M. De; Hart, A. J. Fabrication, Densification, and Replica Molding of 3D Carbon Nanotube Microstructures. *J. Visualized Exp.* **2012**, e3980.